Bulgarian Chemical Communications, Volume 47, Number 2 (pp. 699 – 705) 2015

Controlled aggregation of gold nanoparticles in a di-ureasil matrix. Optical and micro indentation investigation

M. P. Slavova[1,2*], G. I. Zamfirova[3], V. I. Boev[1], V. T. Gaydarov[4], L.K. Yotova[1], M.J.M. Gomes[5], C. J. R. Silva[6]

[1] *Institute of Electrochemistry and Energy Systems, Bulgarian Academy of Sciences, Sofia, BULGARIA*
[2] *Department of Biotechnology, University of Chemical Technology and Metallurgy, Sofia, BULGARIA*
[3] *Department of Machine Elements and Chemistry, University of Transport., Sofia, BULGARIA*
[4] *Department of Electrical Engineering and Physics, University of Transport., Sofia, BULGARIA*
[5] *Centre of Physics, University of Minho, Braga, PORTUGAL*
[6] *Centre of Chemistry, University of Minho, Braga, PORTUGAL*

Received June 19, 2014, Accepted August 13, 2014

Nanocomposite materials with an organic-inorganic urea-silicate (di-ureasil) based matrix containing gold nanoparticles (NPs) were synthesized and characterized by optical (UV/Vis) spectroscopy and indentation measurement. The urea silicate gels were obtained by reaction between silicon alkoxyde modified by isocyanate group and polyethylene glycol oligomer with amine terminal groups in presence of catalyst. The latter ensures the successful incorporation of citrate-stabilized gold NPs in the matrix. It is shown that using a convenient destabilizing agent ($AgNO_3$) and governing the preparative conditions, the aggregation degree of gold NPs can be controlled.
The developed synthesis procedure significantly simplifies the preparative procedure of gold/urea silicate nanocomposites, compared to the procedure using gold NPs, preliminary covered with silica shells. Mechanical properties of the prepared sample were characterised using depth sensing indentation methods (DSI) and an idea about the type of aggregation structures was suggested.

Keywords*:* Nanocomposite; Di-ureasil matrix; Gold nanoparticles; Nanoparticles aggregation; Sol-gel

INTRODUCTION

Producing nanocomposite functional materials for optical applications has attracted much attention in the last decade. Among different optical functionalities, metal NPs offer a great potential for applications in nonlinear optical devices, such as ultrafast optical switches and filters, and for uses as catalysts or sensors. The transfer of NPs into solid substrates while retaining the characteristic properties of single particles, i.e., preventing aggregation, is an important technological task which has to be solved in manufacturing practice.

The matrix itself must satisfy a number of requirements such as a high optical transparency in the visible range, mechanical, and chemical stability. Sol-gel process provides a straightforward and versatile fabrication method for the production of a large number of transparent glassy-like substances. The advantages of this process are low processing temperature, high purity of precursors, good uniformity, reproducibility of the composition and processability. Highly transparent hybrid organic-inorganic structures, where organic and inorganic components are bonded through strong chemical bonds, were prepared by this method. Typical representatives of the covalently linked organic-inorganic materials are the so-called urea silicates or di-ureasils. Optically clear and elastic organic-inorganic di-ureasil nanocomposites containing gold NPs, stabilized by uniform silica shell were produced by mixing preformed NPs colloidal dispersions with urea silicate neat monomer prior to sol-gel transition. The silica shell was used to maintain the colloidal stability during the processes of hydrolysis and condensation [1].

Recently, we have established a procedure, allowing us to embed gold NPs, stabilized by pure electrostatic forces, thus avoiding the stage of covering the NPs with protected silica shells. This approach simplifies the manufacturing of the metal-doped urea silicates as the growth of silica shells around the metal NPs is a delicate and rather time consuming operation. Furthermore, the use of a convenient destabilizing agent ($AgNO_3$) permitted us to control the aggregation degree of gold NPs. In that way we can produce gold/ureasilicate nanocomposites with different absorption profiles, as the formation of large aggregates causes irreversible changes in their optical properties.

* To whom all correspondence should be sent:
E-mail: mslavova@bas.bg

In this work we present the preparation procedure of di-ureasil nanocomposites with embedded citrate-stabilized gold NPs. The reliable preservation of the nanoparticles in the matrix is confirmed by optical absorption measurements and indentation characteristics. It is shown that metal NPs, embedded in the ureasilicate matrix could be fixed at different aggregation stages by controlling the concentration of the aggregation agent in the reaction medium.

EXPERIMENTAL

Materials

O,O-bis(2-aminopropyl)-polypropylene glycol-block-polyethylene glycol-block-polypropylene glycol-500 (Jeffamine ED-600, Fluka) was dried under dynamic vacuum before use. 3-Isocyanate propyl-3-ethoxysilane (ICPTES, Aldrich), tetrachloroauric acid (Aldrich), 3-sodium citrate dihydrate (Aldrich), absolute ethanol (Riedel-de Haën), citric acid monohydrate (Merck) were used as received. Distilled water with a resistance around 18 MS/cm was used for the preparation of dilute aqueous solutions.

Preparation of samples

Urea-silicate neat monomer was prepared by mixing 0.936 mmol Jeffamine ED-600 and 1.870 mmol of ICPTES under stirring. Spherical gold NPs (15 nm) were prepared by boiling 5×10^{-4} M $HAuCl_4$ aqueous solution in the presence of 1.6×10^{-3} M sodium citrate aqueous solution, for 15 min [2]. Later, citric acid in ethanol solution, served as a catalyst for the sol-gel process, citric-stabilized Au colloid solution, and aggregation agent ($AgNO_3$ aqueous solution) were added to the liquid monomer. Table 1 shows the amount of $AgNO_3$ used for the preparation of the samples.

The mixtures were transferred to polystyrene cuvettes and dried in an oven at 40ºC for 48 h. Finally, transparent, free of cracks samples with a base of 21 mm^2 and height of 7 mm were obtained. A photograph of the samples is presented in Fig. 1.

Fig. 1. Au/urea silicate samples with different degree of Au NPs aggregation.

Depth-sensing indentation method

The method known as either depth-sensing indentation (DSI) or instrumented indentation testing (IIT) is based on the experimental measured indentation curves (relationship between the test force and indentation depth) (ISO 14577-1).
The following micro indentation characteristics ware determined (ISO 14577-1) [3]:

$$\text{Dynamic hardness: } HMV = a\,F/h^2, \quad (1)$$

where (F) is the value of the instant load in a loading and unloading testing regime, (a = 3.8584) is a constant which depends on the shape of the indenter and (h) is the indentation depth. This characteristic reveals how the material responds to total deformation during the indentation test including plastic, elastic and viscoelastic deformation components.

– Martens hardness was determined from the slope of the increasing force/indentation depth curve in the 50% ÷ 90% P interval and characterises the material resistance against the penetration (P is the maximum applied load):

$$HMs = 1/(26.43\ m^2), \quad (2)$$

This characteristic has similar physical sense as dynamic hardness, but characterises the material properties at the maximum indentation depth at constant load.

– Indentation hardness is a measure for the material resistance to permanent deformation.

$$Hit = P/24.50h_c^2, \quad (3)$$

where (h_c) is the so called "contact depth" which means the imprint depth when there is a contact between the indenter and the surface of the test piece.

– Microhardness profiles are dependences of Vickers hardness on the applied load (P), or on the penetration depth (h), respectively.

$$HV=f(P);\ \ HV=f(h), \quad (4)$$

– Indentation Elastic Modulus calculated from the unloading part of the dependence by using the equation:

$$1/E_r = (1-\nu_s^2)/Eit + (1-\nu_i^2)/E_i, \quad (5)$$

where (E_r) is the experimental converted elastic modulus based on indentation contact, (ν_s) is the Poisson ratio of specimen, whereas (E_i) and (ν_i) are the Young's modulus and Poisson's ratio for the indenter, respectively.

– Indentation creep which is a relative change in the indentation depth at constant test force:

$$Cit = (h_2 - h_1)/h_1 \qquad (F = const.), \quad (6)$$

where (h_1) and (h_2) are indentation depths at the beginning and the end of the creep measurement [4].

The tests were provided on the dynamic ultra microhardness tester DUH-211S. All measurements were performed at room temperature and the test regime was: loading with a constant loading speed of 0.2926 mN/s till 3 mN, then holding this load for 1 min and then unloading. For viscoelastic materials the relationship between load and depth of penetration is not linearly dependent. That is, for a given load the resulting depth of penetration may depend upon the rate of load application, as well as on the magnitude of the load itself. Ten measurements were made for each sample.

RESULTS AND DISCUSSION

The optical properties of a colloidal dispersion of spherical particles with a radius R can be described by Mie theory, who first explained the origin of the red color of gold colloids [5].
In a dilute colloidal solution containing *N* particles per unit volume (cm^3), the measured absorbance over the path length *d* is:

$$A = \log_{10}\frac{I_0}{I(d)} = \frac{NC_{ext}d}{2.303}, \quad (7)$$

where C_{ext} is the extinction cross-section of a single particle, d is path length and I_0 and *I(d)* are incoming and transmitted light intensities.
For a spherical particle with radius *R*, much smaller than the wavelength of light only the dipole oscillation contributes significantly to the extinction cross-section (dipole approximation) and C_{ext} can be written as the following relationship [6]

$$C_{ext} = \frac{24\pi^2 R^3 \varepsilon_m^{3/2}}{\lambda}\frac{\varepsilon''}{(\varepsilon'+2\varepsilon_m)^2+\varepsilon''^2}, \quad (8)$$

where ε' and ε'' are the real and imaginary part of the wavelength dependent dielectric function and ε_m is the dielectric function of the medium.

Fig. 2 presents the experimental absorption spectrum of the initial aqueous solution of citrate-stabilized gold NPs with an average size of 15 nm, the experimental spectrum of the solid di-ureasil monolith doped with gold NPs, prepared without addition of the aggregation agent (sample 1) and the theoretical spectrum, calculated for the sample 1. The former one is based on eq. 2 utilizing the real and imaginary parts of the dielectric function for bulk gold [7].

There is an expected shift in the position of the plasmon peak obtained for the sample 1 (situated at 529 nm) with respect to the initial colloidal solution in water (located at 519 nm). This is due to a refractive index increase when changing the dispersion medium from ethanol (n = 1.33) to di-ureasil (n = 1.508) The plasmon peak position obtained for sample 1 is in coincidence with the calculated one obtained by using the data for dielectric constant of Johnson and Christy and refractive index of the urea silicate matrix (1.508). It is obvious that the optical response of the prepared nanocomposite resembles that of the starting colloid in the range of plasmon band.

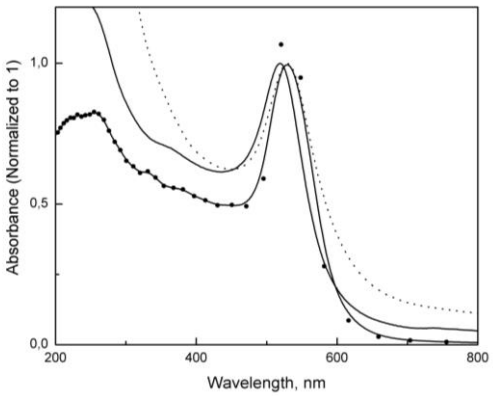

Fig. 2. Experimental absorption spectrum of the initial gold colloid in water (——), experimental absorption spectrum of sample 1 (·····) and calculated absorption spectrum of sample 1 (−•−•−). The calculated spectrum is B-spline connected.

Absorption spectra of the samples containing gold NPs with different degree of aggregation are presented in Fig. 3. Numbers over the curves correspond to the samples designation, presented in the Table 1.

Table 1. Amount of $AgNO_3$ used for the samples preparation.

Samples designation	Molar content of $AgNO_3$, added to the reaction mixture [nmol]
1	–
2	88.5
3	111
4	150
5	177

It is seen from Fig. 2 that with increase of $AgNO_3$ concentration the first plasmon maximum at about 520 nm is broadening and the second maximum at ~700 nm appears and is getting more pronounced. It is clear that gold NPs, embedded in the matrix, undergo changes in color upon the process of aggregation due to the coupling interactions between the surface plasmon fields of the particles [8]. Appearance of longitudinal mode can be explained by formation of dimers and aggregates of higher order, which do not have spherical symmetry and can be roughly represented by equivalent ellipsoids.

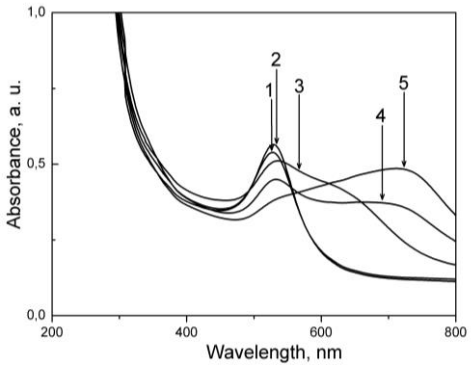

Fig. 3. Absorption spectra of the urea silicate nanocomposites with different degree of NPs aggregation.

Fig. 4 presents the indentation curves (Load – Indentation depth) for all samples. It can be seen that the curves of the loading and unloading are substantially parallel, which means that the samples are extremely elastic.

Fig. 5 shows the generalized arithmetic average of measured indentation characteristics for the studied samples. The lines between the points are only for visual facilitation of the trends.

From Figs. 5 a) and b) it becomes clear that the microindentation parameters change on adding $AgNO_3$. The first portion decreases HMV, HMs and indentation elastic modulus Eit, while micro hardness characteristics Hit and HV* increase. Taking into account that HMV and HMs characterize the total resistance against the penetration and Hit and HV* – the resistance only against plastic deformation it could be concluded that resistance against elastic deformation decreases or the sample becomes more elastic. The next additions of $AgNO_3$ lead to improving all studied characteristics (Fig. 5a), b) and c) till 150 nmol (sample 4). Knowing that the quantity of the gold NPs is the same for all samples, the changes in mechanical properties could be attributed only to arising of different aggregation structures as a consequence of $AgNO_3$ addition. There are many publications dealing with the type of aggregation structures of gold NPs according to the type and quantity of aggregation agent: filamentary, racemose or cross-linked structures [9-11]. Moreover, the gold particles keep their individuality in the aggregates. We suppose that in our case the first portion of $AgNO_3$ partially destroys the stabilizing layer on the gold particles leading to the formation of loose cross-linked structure of gold particles. Obviously, the electrostatic forces between the particles are strong enough to improve the elasticity of the sample. Further $AgNO_3$ addition results in a more complete destruction of the charged surface layer and more complete multilateral linking between the particles, making the cross-linked structure denser. Mechanical properties are improved. At a concentration of destabilizing agent higher than that in sample 4, the aggregation processes are so pronounced that the cross-linked structure is torn and regrouped in a denser cluster or racemose structure. The racemose formations so obtained do not have so much resistance as the cross-linked structure and microindentation characteristics decrease.

Addition of $AgNO_3$ has practically no influence on the creep processes (Fig.5 d). Ground for such interpretation of the micromechanical results gives us the research and TEM micrographs of aggregates of gold nanoparticles published in [10] (Fig. 6) and [11] (Fig. 7 b) for 500 seconds of electron-beam exposure inside a TEM liquid cell at 200 kV. Scale bar: 200 nm.

It can be assumed that the aggregation process starts in a small volume with a higher local concentration of $AgNO_3$ solution, just after its addition. When the solution is homogenized, the global concentration of $AgNO_3$ drops and the aggregation stops. More dilute solution of $AgNO_3$ results in a smaller degree of aggregation. Simultaneously, the viscosity of the urea silicate monomer rapidly increases within a short period of time, fixing the formed aggregates in the urea silicate gel.

CONCLUSIONS

Gold NPs stabilized by pure electrostatic forces were successfully introduced in the urea silicate matrix, avoiding the stage of covering the NPs with protected silica shells and a highly transparent monolith was obtained.

Using a common gold colloidal solution containing particles with unique size and shape and governing the preparative conditions, di-ureasil nanocomposites containing gold NPs aggregates were produced. The arrested aggregation of gold NPs was previously achieved in gelatin films [8]. However, this was obtained for the first time in highly transparent monolith samples.

Micromechanical characteristics change according to the type of aggregation structure. We suppose that the improvement of elastic indentation modulus and resistance against total and plastic deformation is due to the cross-linked structure formed by the gold NPs.

When the metal nanoparticles form racemose structures the mechanical properties slightly decrease.

This approach could be a promising way for the development of flexible filters with desired absorption profile and improved mechanical properties on the basis of immobilized metal fractal aggregates.

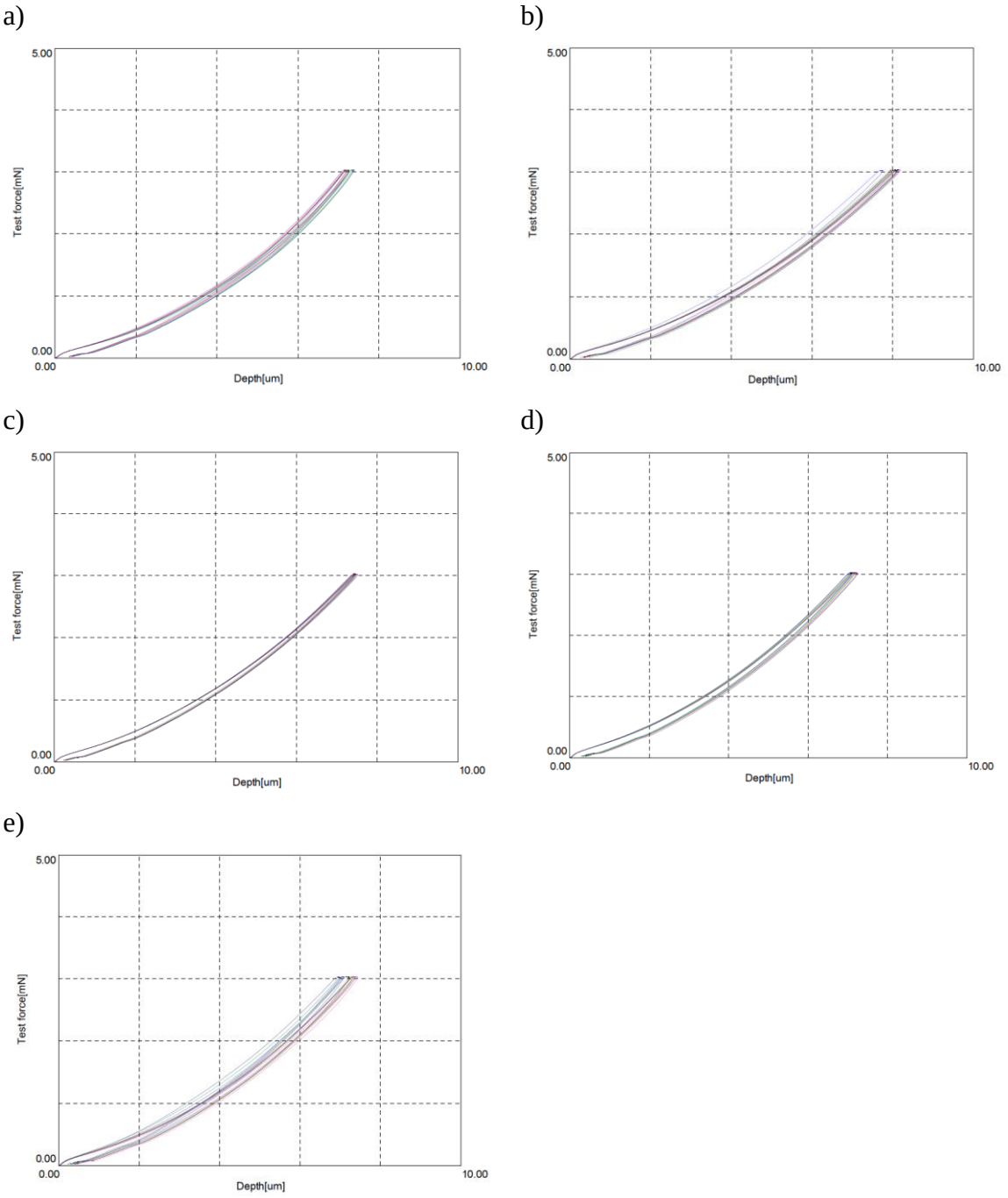

Fig. 4. Load/unload displacement curves: a) sample 1; b) sample 2; c) sample 3; d) sample 4; e) sample 5

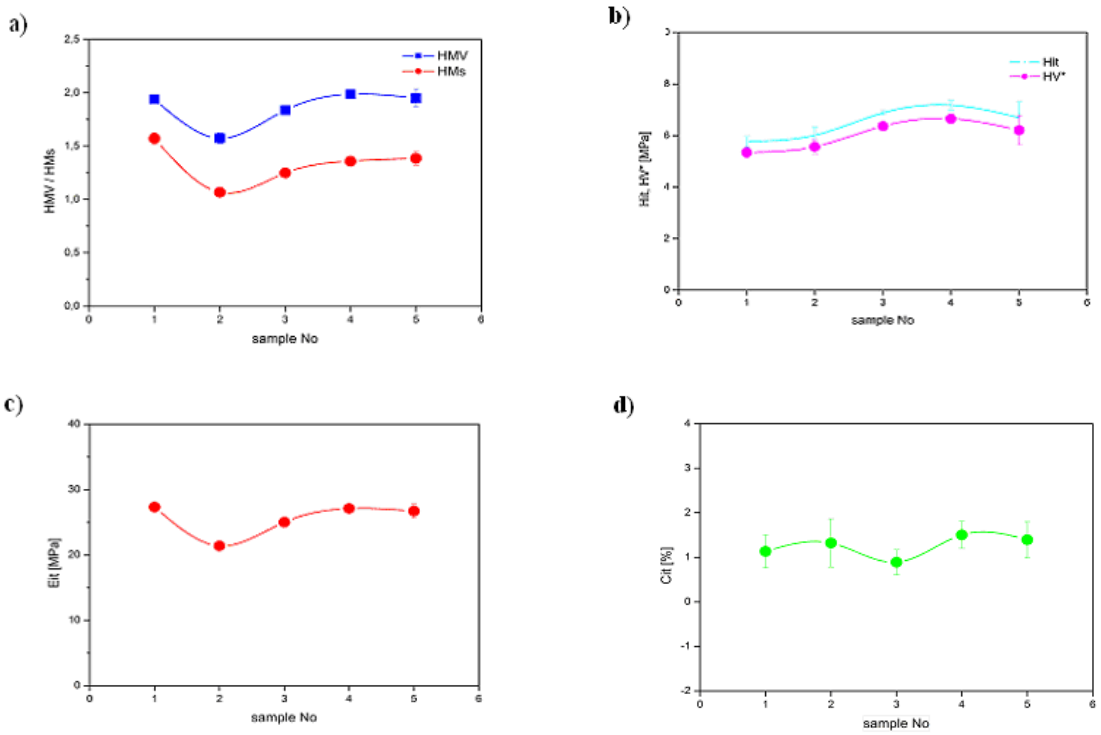

Fig. 5. a) Dynamic microhardness and Martens microhardness; b) Indentation microhardness and Vickers hardness; c) Indentation Elastic Modulus; d) Indentation creep

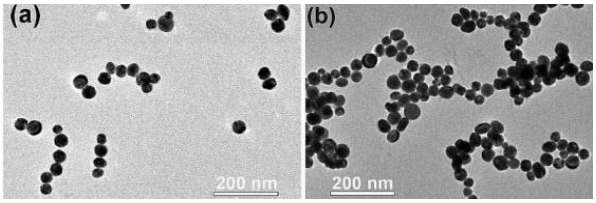

Fig. 6. Cetyl-3-methylammonium-ion-coated gold nanoparticles before (a) and after aggregation

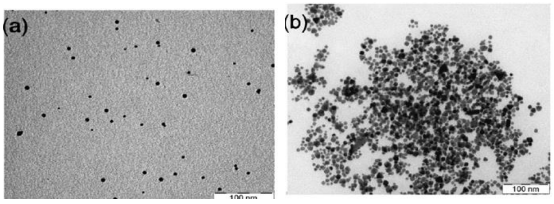

Fig. 7. TEM micrographs of I (a) and II (b) gold NPs samples used for the synthesis of nanocomposites, scale bar: 100 nm

REFERENCES

1. V. I. Boev, J Pérez-Juste, I Pastoriza-Santos, CJR Silva, MJM Gomes, LM Liz-Marzán, *Langmuir*, **20,** 10268 (2004).
2. J, Turkevich, P. C. Stevenson, J. Hiller, *Discuss. Farad. Soc.* **11,** 55 (1951).
3. *ISO/FDIS* 14577-1:2013(E).
4. G. Zamfirova, V. Gaydarov, *Proc.* 8th Intern. Congress "Machines, Technologies, Materials" Varna, Bulgaria, 2011, p 73.
5. G. Mie, *Ann. Phys.*, **25,** 329 **(**1908).
6. P. Mulvaney, *Langmuir*. **12.** 788 (1996).
7. P. B. Johnson, R. W. Christy, *Phys. Chem. B*, **6**, 4370 (1972).
8. M. Quinten, D. Schoenauer, U. Kreibig, *Z. Phys. D*, **26**, 239 (1989).
9. J. Turkevich, G. Garton, P. C. Stevenson, *J. Colloid Sci. Suppl.*, **9,** 26 (1954).
10. Y. Liu, X. M. Lin, Y. Sun, T. Rajh, *J. Am. Chem. Soc.*, **135**, 3764 (2013).
11. I. Pardinas-Blanco, C. E. Hoppe, M. A. Lorpez-Quintela, J. Rivas, *J. Non-Cryst. Sol.*, **353**, 826 (2007).

КОНТРОЛИРАНО АГРЕГИРАНЕ НА ЗЛАТНИ НАНОЧАСТИЦИ В ДИУРЕАСИЛАТНА МАТРИЦА. ОПТИЧНО И МИКРОИДЕНТАЦИОННО ИЗСЛЕДВАНЕ

М. П. Славова[1,2*], Г. И. Замфирова[3], В. И. Боев[1], В. Т. Гайдаров[4],
Л. К. Йотова[2], М. Д. М. Гомес[5], К. Д. Р. Силва[6]

[1] Институт по електрохимия и енергийни системи, Българска академия на науките, София, България
[2]Катедра биотехнологии, Химикотехнологичен и металургичен университет, София, България
[3] Катедра машинни елементи, материалознание и химия, Висше транспортно училище, София, България
[4] Катедра електротехника и физика, Висше транспортно училище, София, България
[5] Център по физика, Университет Миньо, Португалия
[6] Център по химия, Университет Миньо, Португалия

Получена на 19.07. 2014, Приета на 13.08.2014

(Резюме)

Нанокомпозитни материали с органично-неорганична карбамид-силикатна матрица (ди-уреасили), съдържаща златни наночастици (НП), са синтезирани и характеризирани с оптична (UV/ Vis) спектроскопия и индентационни измервания. Силикатните урея гелове са получени чрез реакция между силициев алкоксид модифициран с изоцианатна група и олигомер полиетилен гликол с аминни крайни групи в присъствие на катализатор. Последният гарантира успешното включване на цитрат стабилизирани златни НП в матрицата. Показано е, че степента на агрегация на златните НП може да се контролира с помощта на подходящ дестабилизиращ агент ($AgNO_3$) и промяна в условията на получаване.

Разработената процедура за синтез значително опростява подготвителна процедура на златото/ урея силикатни нанокомпозити, в сравнение с процедурата за използване на предварителна покрити с кварцови черупки златни НП. Механичните свойства на приготвената проба са охарактеризирани с помощта на измерване на дълбочинно проникващ индентационен метод (DSI) и е направено предположение за вида на агрегационните структури.